Potential Energy Surfaces of Si_mO_n Cluster Formation and Isomerization

Pavel V. Avramov,[†,‡] Ivana Adamovic,[†] Kai-Ming Ho,[†] C. Z. Wang,[†] W. C. Lu,[†] and Mark S. Gordon*[,†]

Ames National Laboratory/Department of Chemistry, Iowa State University, Ames, Iowa 50011, and L.V. Kirensky Institute of Physics SB RAS, Academgorodok, 660036, Russia

Received: March 2, 2005; In Final Form: April 26, 2005

The reaction paths for formation and isomerization of a set of silica Si_mO_n ($m = 2,3$, $n = 1-5$) nanoclusters have been investigated using second-order pertubation theory (MP2) with the 6-31G(d) basis set. The MP2/6-31G(d) calculations have predicted singlet ground states for all clusters excluding Si_3O_2. The total energies of the most important points on the potential energy surfaces (PES) have been determined using the completely renormalized (CR) singles and doubles coupled cluster method including perturbative triples, CR-CCSD(T) with the cc-pVTZ basis set. Although transition states have been located for many isomerization reactions, only for Si_3O_3 and Si_3O_4 have some transition states been found for the formation of a cluster from the separated reactants. In all other cases, the process of formation of Si_mO_n clusters appears to proceed without potential energy barriers.

I. Introduction

Si_mO_n clusters have played a key role in the synthesis of silicon nanostructures. One-dimensional silicon−silica and silicon−carbon−silica nanowires and nanotubes of various shapes and structures have been synthesized under high-temperature conditions.[1−5] Bulk-quantity Si nanowires[1,2] have been synthesized by thermal evaporation of powder mixtures of silicon and SiO_2 or by thermal evaporation of silicon monoxide.[3] Initially, SiO vapor is generated from a powder mixture and condensed on the substrate, with Si nanoparticles and nanowires surrounded by shells of silicon oxide. The silica content in the starting Si/SiO_2 reaction mixture appears to be a key factor in nanowire growth and structure.[1,2] Surface thin Si_xO structures function as catalysts on the tips and form SiO_2 structures, which retard the lateral growth of the nanowires. It has also been demonstrated[3] that SiO can contribute to the formation of SiC multiwall nanotubes and nanowires and SiC−SiO_x nanowires in thermochemical reactions with multiwall carbon nanotubes.

The structures and properties of Si_mO_n clusters have therefore been studied intensively by photoelectron spectroscopy[6−9] and by several theoretical approaches.[7,9−20] On the basis of the vibrationally resolved PES spectra, Si_3O_3 and Si_3O_4 clusters are proposed to have closed-shell electronic structures.

The experimental studies have been accompanied by theoretical quantum-chemical calculations[7,9] on a set of $Si_mO_n^-$ and Si_mO_n clusters using second-order perturbation theory (MP2)[21] and the 6-311+G(d) basis set.[22] This combination of experiments and quantum-chemical calculations allowed the authors to interpret the main features of the PES spectra and to extract the adiabatic electron affinities of neutral Si_mO_n clusters.

Previous theoretical studies have predicted the atomic structures of $Si_mO_n^-$ and Si_mO_n clusters[7−10,14−16,18,19] at various levels of theory. These include density functional theory (DFT)[10,14,16,19] and such correlated ab initio approaches as MP2, multireference second-order perturbation theory, quadratic configuration interaction (QCISD(T)), and coupled cluster (CCSD(T)) methods.[7−9,15,18] Several differences among these methods are apparent, even in the lowest-energy spin state of some Si_mO_n clusters, as well as in the equilibrium geometry of the complexes. For example, a recent study[19] predicted a singlet electronic ground state for the pyramidal global minimum of Si_3O_2, in contrast with earlier results[9,18] in which a triplet global minimum was predicted for the flat pentagon structure. This can be attributed to the importance of electron correlation in correctly predicting the electronic structure of silica clusters.[20]

The reactivity and cohesion energies[13] of a set of Si_mO_n ($n,m = 1-8$) clusters and reaction paths for assembling Si_mO_n clusters have also been studied.[19] Zhang et al.[13] have used the B3LYP functional[23] with the 6-31G(d) basis set, as well as the G2MP2 method.[24] Adamovic and Gordon[20] employed multireference perturbation theory and CCSD(T) extrapolated to the complete basis set limit to study the competing $Si + O_2$ reactions on the singlet and triplet surfaces. All of these studies showed that dynamic correlation clearly plays an important role in such systems. The aim of the present paper is to study structures, transition states, relative energies, and formation reaction paths at the MP2 and CCSD(T) levels of theory for Si_2O_2, Si_2O_3, Si_2O_4, Si_3O, Si_3O_2, Si_3O_3, and Si_3O_4 clusters.

Although some of the species considered in the present work have been discussed previously, there has not been a comprehensive study of these systems. Some theoretical studies[25] considered the structures and vibrational spectra of SiO and Si_2O_2. The SiO dimer is postulated to be a ring species with D_{2h} symmetry.[26] Most theoretical studies on Si_2O_3 have been concerned with the high-energy, multiconfigurational, propellane-like structure, in which the Si atoms are connected by three bridging O atoms.[27−29] The global minimum Si_2O_3 structure was found to have an O atom bound to rhombic Si_2O_2, both in the experimental work of Wang et al.[30] and in a recent comprehensive theoretical study by Lu et al.[19] The geometry, energy, and vibrational frequencies, at the Hartree−Fock level of theory, were determined for the D_{2h} global minimum and C_{2v} transition

* Corresponding author. E-mail: mark@si.fi.ameslab.gov.
† Iowa State University.
‡ L.V. Kirensky Institute of Physics SB RAS.

10.1021/jp058078v CCC: $30.25
Published on Web 06/28/2005

state of Si_2O_4 in a study by Ystenes.[31] The D_{2h} structure was also found to be the global minimum in the recent study by Lu et al.[19]

Presented here is a systematic investigation of the growth reactions for the family of Si_mO_n ($m = 2-3$, $n = 1-4$) species. This study is organized as follows: Section II describes the computational methods, followed by results and discussion in Section III. Conclusions are presented in Section IV.

II. Computational Details

To calculate the electronic structure of silica nanoclusters, the general atomic and molecular electronic structure system (GAMESS)[32] code has been used. Geometry optimizations and transition state searches have been performed using the MP2/6-31G(d) level of theory; for isomer **3** of Si_2O_3, density functional theory (DFT)[33] using the B3LYP functional was also employed.[33] Coupled cluster calculations have been performed at the MP2/6-31G(d) geometries using the completely renormalized coupled cluster approach with singles, doubles, and perturbative triples (CR-CCSD(T))[34] with the correlation consistent cc-pVTZ basis set[35,36] to obtain improved energies of all minima and transition states. Because isomer **3** of Si_2O_3 is very configurationally mixed, multireference second-order perturbation theory (MRMP2)[37] was also used to obtain energy corrections for this species.

All transition states and minima have been confirmed by the calculation and diagonalization of the appropriate Hessian matrix (matrix of energy second derivatives). For DFT and MP2, Hessians were obtained by taking finite differences of analytic gradients. TCSCF analytical Hessians can be obtained using the corresponding generalized valence bond (GVB)[38] method. The reaction enthalpies were corrected for zero-point energy (ZPE) and temperature effects.

The intrinsic reaction coordinate (IRC) method has been employed with the Gonzales−Schlegel second-order integration method[39] to ensure that each transition state joins two appropriate local minima along the potential energy surface. A useful diagnostic to assess the multireference nature of unusual structures is to examine the MP2 natural orbital occupation numbers (NOON).[40] A closed-shell, single configuration is indicated by NOON that are ∼2.0 and 0.0 for occupied and virtual orbitals, respectively. Significant deviations from these values (∼0.1) indicate some degree of multireference character in the wave function.

III. Results and Discussion

(a) SiO + SiO → Si_2O_2. Since all molecules involved in this reaction are closed-shell (Hartree−Fock like) systems, single reference methods were used for all of the calculations. Optimizations were accomplished with MP2/6-31-G(d), and energy corrections were taken into account with CCSD(T)/cc-pVTZ. Figure 1 gives a schematic of reaction (a) and reactant and product structures. The lowest-energy product has D_{2h} symmetry, in agreement with previous studies. Other isomers were not considered, since they are much higher in energy. An MP2 optimization initiated with two SiO molecules ∼3 Å apart, as represented in Figure 1, goes directly into the D_{2h} isomer of Si_2O_2, with no intervening barrier. The MP2/ 6-31G(d) reaction enthalpy with ZPE and temperature corrections is $\Delta H_{298.15} = -38.4$ kcal/mol, while the CCSD(T)/cc-pVTZ $\Delta H_{298.15} = -49.5$ kcal/mol. The experimental enthalpy of this dimerization reaction[43] is $\Delta H_{exp}^{298.15} = -48.5$ kcal/ mol, so the experimental and CCSD(T)/cc-pVTZ results are in good agreement. The discrepancy between CCSD(T)/cc-pVTZ and MP2/6-31G(d) reaction enthalpies emphasizes the importance of triple excitations for a proper treatment of dynamical correlation effects in the silicon−oxygen systems.

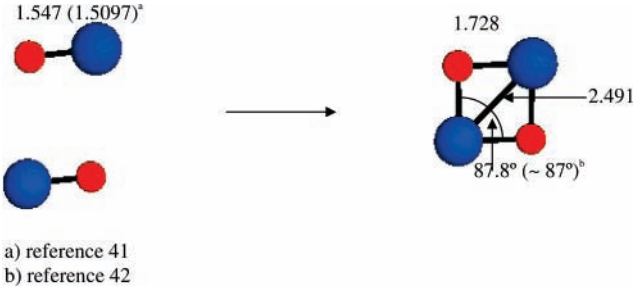

Figure 1. A schematic of reaction (a): SiO + SiO → Si_2O_2; MP2/6-31G(d) structural parameters for reaction (a) (Å).

TABLE 1: Relative Energies of the Si_2O_3 Isomers (kcal/mol) (CCSD(T) and CR-CCSD(T) with cc-pVTZ Basis Set, All Others with 6-31G(d) Basis Set

	HF	DFT	MP2	MCSCF	CCSD(T) (CR-CCSD(T))
1 (open)	0.0	0.0	0.0	0.0	0.0
2 (triangle)	70.2	52.9	51.0	68.5	54.6 (56.3)
3 (tricycle)	86.3	53.9	49.1	52.6	58.0 (61.3)
4 (circle)	71.6	60.0	74.9	72.7	71.9 (72.9)
5 (linear)	91.3	92.7	92.3	125.7	102.1 (108.0)
6 (circle1)	223.0	185.9	208.8	223.1	212.3 (220.5)
7 (open1)	256.4	118.6	228.1	132.3	223.1 (229.7)

(b) SiO + SiO_2 → Si_2O_3. The first step in the investigation of formation of Si_2O_3 was to find all possible candidates for the ground state of Si_2O_3. The propellane-like structure is the only Si_2O_3 isomer that has been extensively examined previously,[27−29] primarily due to its high-energy and multiconfigurational character. A systematic search for all possible Si_2O_3 isomers resulted in the seven structures shown in Figure 2. The global minimum is isomer **1** (open). This is in agreement with Wang et al.[30] and Lu et al.[19]

The relative energies of all seven isomers, using various levels of theory, are given in Table 1. Most of these methods give the same energy ordering, with the open structure being much lower in energy than any other isomer. For the most part, MP2/6-31G(d), CCSD(T)/cc-pVTZ, and CR-CCSD(T)/cc-pVTZ relative energies are in reasonable agreement. The basis set effect (from 6-31G(d) to cc-pVTZ) is usually on the order of ∼3 kcal/mol. The biggest disagreement between MP2 and CC methods occurs for isomers **3** and **5** (∼10 kcal/mol), the two most multiconfigurational isomers. For the tricycle isomer, an MRMP2/6-31G(d) single-point energy correction, at the MCSCF optimized geometry, gives a relative energy of ∼37.7 kcal/mol. This value may be too low, on the basis of the CR-CCSD(T)/cc-pVTZ relative energy of 61.3 kcal/mol.

Analysis of the Hessian matrix shows that the open isomer is a minimum on the potential energy surface at most levels of theory. Although the TCSCF numerical Hessian has one imaginary frequency of 1422 cm^{-1}, the equivalent analytical GVB Hessian has no imaginary frequencies. It is therefore concluded that the TCSCF Hessian has numerical errors, and the GVB analytic Hessian was used for all isomers. All other isomers are minima, except for **6** (circle1), which has one imaginary frequency at all levels of theory except HF, and tricycle with one imaginary frequency at the HF level of theory. The linear isomer does not exist at the HF level (it dissociates to SiO + SiO_2) and has 5, 4, 4, and 2 imaginary frequencies at the DFT, MP2, TCSCF, and GVB levels of theory, respectively.

Next, consider the TCSCF natural orbital occupation numbers (NOON). Significant multiconfigurational character was found

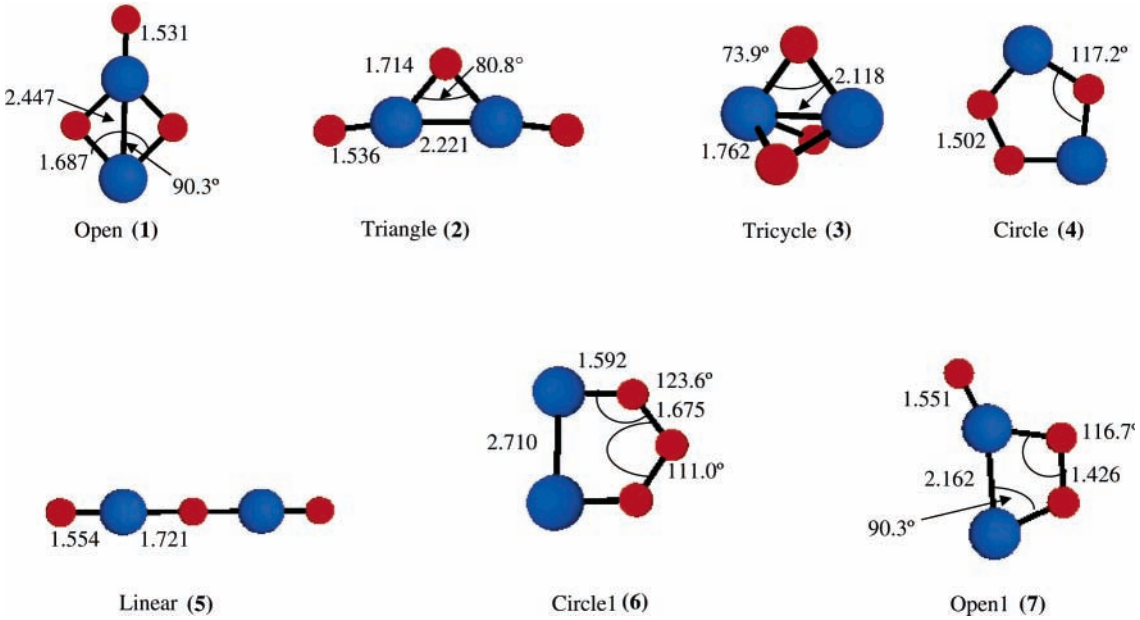

Figure 2. The lowest-energy Si_2O_3 isomers; MP2/6-31G(d) geometry parameters (Å).

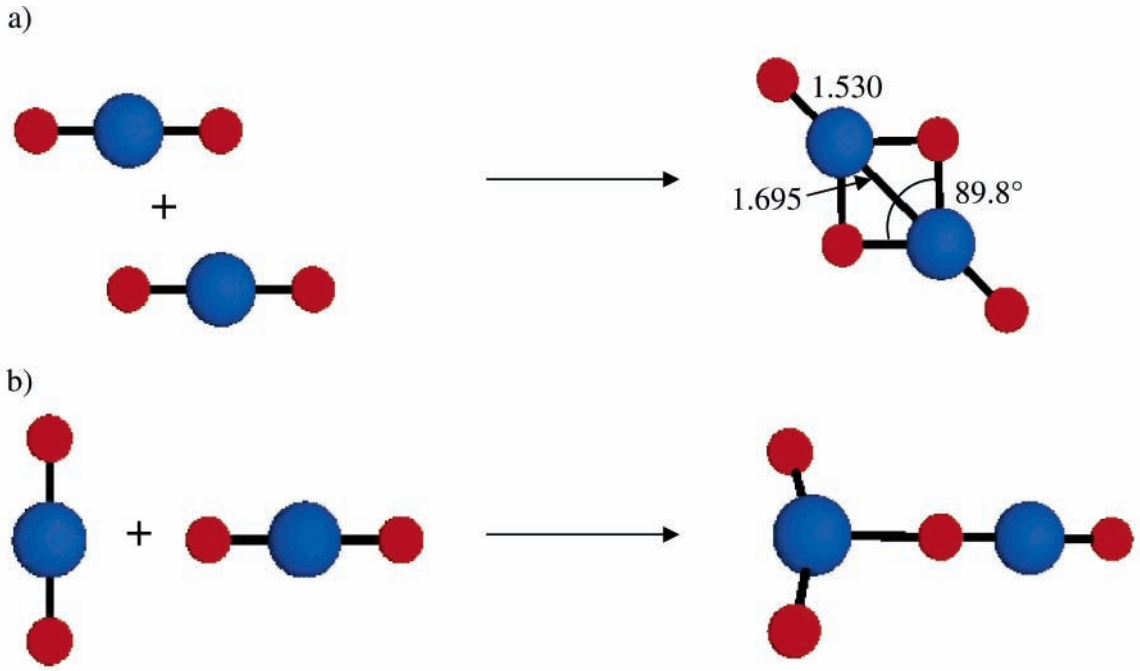

Figure 3. (a) A schematic of the parallel path for reaction (5)—formation of the D_{2h} isomer; MP2/6-31G(d) geometry parameters of the Si_2O_4 D_{2h} isomer (Å). (b) A schematic of the normal path for reaction (5)—formation of the C_{2v} isomer.

just for isomers **3** and **5**. The NOONs of the highest occupied molecular orbital (HOMO) are 1.643 and 1.755, respectively, for isomers **3** and **5**, while corresponding NOONs for the lowest unoccupied molecular orbitals (LUMO) are 0.357 and 0.245.

The reaction path for the formation of Si_2O_3 from SiO and SiO_2 was determined by initiating an MP2 optimization, in C_s symmetry, with SiO and SiO_2 ~5 Å apart. This leads to the formation of the isomer **1** (open) with no barrier. The C_s reaction path avoids the symmetry-forbidden C_{2v} path. The MP2/6-31G(d) reaction enthalpy for the formation of Si_2O_3 from SiO and SiO_2 is $\Delta H_{298.15} = -70.4$ kcal/mol, while the CCSD(T)/cc-pVTZ $\Delta H_{298.15} = -77.2$ kcal/mol.

(c) $SiO_2 + SiO_2 \rightarrow Si_2O_4$. Figure 3 gives the MP2/6-31G(d) geometrical parameters for the Si_2O_4 D_{2h} isomer. A C_{2v} structure lies 79.6 kcal/mol above the global minimum, at the MP2/6-31G(d) level of theory. The CCSD(T)/cc-pVTZ//MP2/6-31G(d) relative energy is 84.0 kcal/mol. The C_{2v} structure has 2 imaginary frequencies, so it is a second-order saddle point. If the C_{2v} structure is optimized in C_s symmetry (breaking C_{2v} symmetry), it goes directly into D_{2h} without any barrier, as found previously.[31]

Figure 3a,b gives schematic representations of two different paths for the formation of Si_2O_4. Initiating an MP2/6-31G(d) optimization in C_s symmetry from the parallel orientation (Figure 3a) leads to the D_{2h} isomer, with no barrier. Starting from the perpendicular orientation (Figure 3b) leads to the C_{2v} isomer. This path is also barrierless. Both paths are highly exothermic. The MP2 (CCSD(T)/cc-pVTZ)) enthalpy of path (a) is $\Delta H^{298.15}{}_{\mathrm{MP2/6-31G(d)}} = -91.5$ (−94.1) kcal/mol. The corresponding enthalpies for path (b) are −11.8 and −13.6 kcal/mol, respectively. Since both reaction paths have no barrier, both C_{2v} and D_{2h} are possible products in the reaction of two SiO_2.

TABLE 2: Structures and Energies of Si_2O_5 Isomers

Isomer[a]	Structure[b] V1	Structure[b] V2	CR-CCSD(T) (MP2) relative energy, kcal/mol	Point Group	MP2 HOMO NOON[c]
GS1			0.0 (0.0)	C_{2v}	1.90
GS2			19.7 (18.7)	C_{2v}	1.93
GS3			31.6 (23.6)	C_{2v}	1.90
GS4			57.6 (59.9)	C_{2v}	1.92
GS5[d]			87.2 (--)	D_{2h}	--

[a] Names of isomers. [b] V1 and V2 are two views of each isomer. [c] MP2 natural orbital occupation numbers. [d] The structure has been determined only at the B3LYP level.

TABLE 3: Structures, Energies, and Reaction Paths of Transition States of Si_2O_5[d]

Transition state[a]	Structure[b] V1	Structure[b] V2	Point Group	MP2 HOMO NOON[c]	GS[i]	GS[f]	Barrier height, (kcal/mol) GS^i/GS^f CR-CCSD(T) (MP2)[e]
TS1			C_s	1.91	GS2	GS1	62.1/81.8 (58.5/77.2)
TS2			C_2	1.91	GS2	GS3	14.7/2.9 (8.8/4.0)
TS3			C_{2v}	1.66	GS2	GS5	52.0/-15.3 (42.9/--)

[a] Names of structures. [b] V1 and V2 are two views of each transition state. [c] MP2 natural orbital occupation numbers. [d] GS^i and GS^f denote initial and final minima on the IRC path. [e] Barrier height from GS^i/GS^f.

However, the global minimum, D_{2h}, is much lower in energy, and the C_{2v} structure is a second-order saddle point. So, the C_{2v} species is dynamically unstable, and vibrations of this structure should easily lead to the global minimum.

(d) Si_2O_5. Closed- and open-shell (S = 1) MP2 6-31G(d) calculations have been performed to determine the nature of the ground state. It is predicted that the global minimum Si_2O_5 structure is a singlet. The singlet−triplet splitting for the global minimum structure GS1 is 23.5 kcal/mol. A set of energy minima and transition states has been determined (Tables 2 and 3, Figure 4) for the singlet ground state. The doubly bridged GS1 isomer appears to be the global minimum on both the MP2 and CR-CCSD(T) potential energy surfaces. The cyclic GS2 isomer is 19.7 (18.7 at the MP2 level) kcal/mol higher in energy than GS1, with GS3 and GS4 considerably higher. Isomers GS1−GS4 have MP2 NOON for the highest occupied molecular orbital (HOMO) in the range 1.90−1.93, reasonably close to the single configuration values of 2.0. It was not possible to determine the MP2 geometry for GS5 because the underlying HF calculations did not converge. Instead, the geometry of this

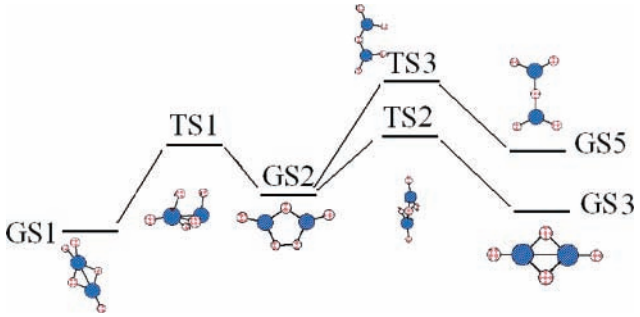

Figure 4. A schematic of the Si_2O_5 isomerization potential energy surface.

TABLE 4: Structures and Energies of Isomers of Si_3O

Isomer[a]	Structure[b] V1	Structure[b] V2	CR CCSD(T) (MP2) relative energy, kcal/mol	Point Group	MP2 HOMO NOON[c]
GS6			0.0 (0.0)	C_{2v}	1.91
GS7			12.4 (14.7)	C_s	1.93
GS8			19.7 (17.2)	C_s	1.91

[a] Names of isomers. [b] V1 and V2 are two views of each isomer. [c] MP2 natural orbital occupation numbers.

structure was determined using DFT/B3LYP. The rather high CR-CCSD(T) relative energy for this species was then determined at the B3LYP geometry.

Transition states connecting the minima in Table 2 are listed in Table 3. TS3 has the smallest MP2 NOON for the HOMO. This may explain why the reverse barrier for TS3 disappears when single-point CR-CCSD(T) calculations are performed at the MP2 geometry. Another reason may be the use of the B3LYP GS5 geometry.

Note that all transition states listed in Table 3 correspond to isomerization reactions. A wide search for transition states, intermediates, and IRC calculations has led to the conclusion that no barriers exist for the formation of Si_2O_5 from $SiO_2 + SiO_3$, even though several possible pathways have been explored. Indeed, an MP2 optimization initiated with separated reactants ($SiO_2 + SiO_3$) ~4 Å apart goes directly to the GS1 structure with no barrier. The CR-CCSD(T) ΔE for the reaction $SiO_2 + SiO_3 \rightarrow Si_2O_5$ is −102.5 kcal/mol. The corresponding MP2 value is −101.3 kcal/mol.

The global minimum GS1 can isomerize to GS2 through transition state TS1, with heights of forward and reverse CR-CCSD(T) barriers of 81.8 and 62.1 kcal/mol, respectively. GS2 can isomerize to GS5 and GS3 via transition states TS3 and TS2, respectively. Breaking the O−O bond via TS3 and creation of an equivalent O−O bond from the other side of the molecule generates an equivalent GS2 structure.

(e) Si_3O. Closed- and open-shell (S = 1) MP2 6-31G(d) geometry optimizations have been performed to determine the nature of the ground electronic state. It is predicted that the Si_3O global minimum is a singlet, with a singlet−triplet splitting of 40.9 kcal/mol. The Si_3O energy minima and transition states for the singlet ground state are shown in Tables 4 and 5, respectively. A schematic of the potential energy surface is given in Figure 5. GS6 is predicted by both MP2 and CR-CCSD(T) to be the global minimum on the singlet surface, with CR-

TABLE 5: Structures, Energies, and Reaction Paths of Transition States of Si_3O[d]

TS[a]	Structure[b] V1	Structure[b] V2	Point Group	MP2 HOMO NOON[c]	GS[i]	GS[f]	Barrier height, (kcal/mol) GS[i]/GS[f] CR-CCSD(T) (MP2)[e]
TS4			C_s	1.94	GS7	GS6	13.4/25.8 (17.9/32.6)
TS5			C_s	1.91	GS6	GS8	24.2/4.5 (21.2/4.1)

[a] Names of structures. [b] V1 and V2 are two views of each transition state. [c] MP2 natural orbital occupation numbers. [d] GS[i] and GS[f] denote initial and final minima on the IRC path. [e] Barrier height from GS[i]/GS[f].

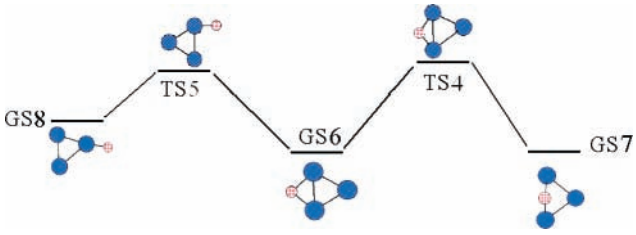

Figure 5. A schematic of the Si_3O isomerization potential energy surface.

CCSD(T) relative energies of 12.4 and 19.7 kcal/mol, respectively, for GS7 and GS8. All three isomers have MP2 HOMO NOON greater than 1.9, suggesting that they are close to closed-shell species.

All transition states listed in Table 5 have MP2 NOON greater than 1.9. The search for transition states, intermediates, and IRC calculations suggests that no barriers exist for the reaction SiO + Si_2 → Si_3O. The MP2 optimization initiated with reactants Si_2 + SiO ~4 Å apart goes directly to the GS6 structure with no barrier.

IRC calculations confirm that the global minimum GS6 can isomerize to GS7 via TS4, with a CR-CCSD(T) barrier of 25.8 kcal/mol. The isomerization of GS6 to GS8 via TS5 has a barrier of 24.1 kcal/mol.

(f) Si_3O_2. Closed- and open-shell (S = 1) MP2/6-31G(d) calculations have been performed to determine the nature of the ground electronic state. It has been predicted that the global minimum Si_3O_2 structure is a triplet. Since the CR-CCSD(T) method is currently available only for closed shells, the CR-CCSD(T) calculations were performed only for the singlet states. Since the MP2 and CR-CCSD(T) energy orderings are similar for the other species, MP2 relative energies are also expected to be reliable here. The Si_3O_2 singlet and triplet energy minima and transition states are presented in Tables 6 and 7, respectively. GS15 (S = 1) is predicted to be the global minimum, 6.8 + 4.9 = 11.7 kcal/mol lower in energy at the MP2 level of theory than the corresponding singlet isomer (GS11) and 4.9 kcal/mol lower in energy than the lowest-energy singlet, GS9. One other singlet, GS10, and one other triplet, GS16, have small MP2 relative energies of 11.1 and 16.9 kcal/mol, respectively. Isomers GS9−GS13 (S = 0) have the same energy order at both the MP2 HOMO and CR-CCSD(T) levels of theory. All singlet isomers GS9-GS13 have MP2 NOON in the range of 1.92−1.95, so these are essentially closed-shell species.

The search for transition states, intermediates, and IRC calculations suggests that no barriers exist for the formation reaction (SiO + Si_2O → Si_3O_2) of the singlet GS11 state. Several MP2 optimizations initiated with separated Si_2O + SiO in the singlet state ~4 Å apart go directly to the GS11 structure with no barrier. The CR-CCSD(T) (MP2) energy difference for the reaction Si_2O + SiO → Si_3O_2 = −35.3 (−36.9) kcal/mol. Similarly, GS9 forms with no intervening barrier, starting from SiO + Si_2O, separated by ~3 Å.

The CR-CCSD(T) GS11 → TS6 barrier is negative. This suggests that either the location of the transition state shifts at the higher level of theory or the CR-CCSD(T) barrier does indeed disappear. For the isomerization GS11 → GS10, the MP2 barriers in both directions are very small, ~2 kcal/mol. So, there must be a very flat potential energy surface in this region. For all singlet Si_3O_2 transition states, the MP2 HOMO NOON are in the range 1.91−1.94.

TABLE 6: Structures and Energies of Isomers of Si_3O_2

Isomer[a], multiplicity	Structure[b] V1	Structure[b] V2	CR CCSD(T) (MP2) relative energy (kcal/mol)	Point Group	MP2 HOMO NOON[c]
GS9, S=0			0 (0.0)	C_{2v}	1.94
GS10, S=0			2.2 (6.2)	C_s	1.94
GS11, S=0			13.3 (6.8)	C_{2v}	1.95
GS12, S=0			30.7 (28.3)	C_s	1.92
GS13, S=0			37.7 (38.1)	C_{2v}	1.92
GS14, S=1			-- (21.5)	D_{3h}	--
GS15, S=1			-- (-4.9)	C_{2v}	--
GS16, S=1			-- (12.0)	C_s	--
GS17, S=1			-- (36.3)	C_s	--

[a] Names of the isomers. [b] V1 and V2 are two views of each isomer. [c] MP2 natural orbital occupation numbers.

TABLE 7: Structures, Energies, and Reaction Paths of Transition States of Si_3O_2[d]

Isomer[a], multiplicity	Structure[b] V1	Structure[b] V2	Point Group	MP2 HOMON OON[c]	GS[i]	GS[f]	Barrier height, (kcal/mol) GS[i]/GS[f] CCSD(T) (MP2)
TS6, S=0			C_s	1.94	GS11	GS10	-12.7/1.6 (1.5/2.1)
TS7, S=0			C_1	1.93	GS12	GS10	2.9/31.4 (5.1/27.2)
TS8, S=1			C_1	--	GS15	GS17	--/-- (22.4/5.6)

[a] Names of the structures. [b] V1 and V2 are two views of each transition state. [c] MP2 natural orbital occupation numbers. [d] GS[i] and GS[f] denote initial and final minima on the IRC path.

TABLE 8: Structures and Energies of Isomers of the Si_3O_3 Cluster

Isomer[a]	Structure[b] V1	Structure[b] V2	CR CCSD(T) (MP2) relative energy (kcal/mol)	Point Group	MP2 HOMO NOON[c]
GS18			0.0 (0.0)	D_{3h}	1.95
GS19			36.2 (33.0)	C_s	1.95
GS20			50.6 (45.9)	C_s	1.95
GS21			87.8 (72.0)	C_s	1.94
GS22			90.7 (90.3)	C_{2v}	1.94
GS23			96.9 (84.9)	C_s	1.94
GS24			99.4 (70.9)	C_{2v}	1.95
GS25			138.9 (94.6)	C_{2v}	1.94
GS26			167.4 (168.7)	C_1	1.91
GS27			185.2 (176.0)	C_s	1.91
GS28			193.3 (183.2)	C_1	1.92
IM1[d]			52.1 (41.4)	C_s	1.94

[a] Names of the isomers. [b] V1 and V2 are two views of each isomer. [c] MP2 natural orbital occupation numbers. [d] IM1 indicates SiO + Si_2O_2 intermediate structure.

The MP2 IRC calculations show that GS10 can isomerize to GS11 via transition state TS6 and to GS12 through TS7. It is useful to note that two couples of isomers (GS11 (S = 0)−GS15 (S = 1) and GS12 (S = 0)−GS17 (S = 1)) have similar atomic structures, so that structures could be connected via singlet−triplet crossing involving TS8 (S = 1).

(g) Si_3O_3. The Si_3O_3 energy minima and transition states are presented in Tables 8 and 9, respectively. A schematic of this section of the potential energy surface is shown in Figure 6. Singlet GS18 is the lowest-energy isomer on both the MP2 and CR-CCSD(T) potential energy surfaces, and all other isomers are much higher in energy. The singlet−triplet splitting for the lowest-energy singlet and triplet isomers is 64.2 kcal/mol. All singlet isomers have MP2 HOMO NOON in the range of 1.91−1.95.

For several MP2 transition states (TS9, TS13−TS17), the CR-CCSD(T) barriers are negative. This can mean either that these barriers disappear at the CR-CCSD(T) level of theory or that the position of the transition state undergoes a significant shift. For all TSs, the MP2 HOMO NOON are in the range 1.91−1.95.

TABLE 9: Structures, Energies, and Reaction Paths for Si_3O_3 Transition States[d]

TS[a]	Structure[b] V1	Structure[b] V2	Point Group	MP2 HOMO NOON[c]	GS[i]	GS[f]	Barrier height, (kcal/mol) GS[i]/GS[f] CR-CCSD(T) (MP2)
TS9			C_s	1.95	IM1 (Si_2O_2 + SiO)	GS19	-0.2/15.7 (0.1/8.4)
TS10			C_1	1.93	GS22	GS24	15.2/6.4 (10.9/30.3)
TS11			C_1	1.91	GS27	GS26	10.4/2.3 (9.7/2.4)
TS12			C_1	1.91	GS27	GS28	2.5/20.2 (6.2/13.5)
TS13			C_s	1.94	GS25	Si_2O_2 +SiO	-10.2/15.5 (19.4/10.8)
TS14			C_1	1.93	GS25	GS21	-8.6/42.5 (20.4/43.0)
TS15			C_1	1.92	GS25	GS20	-20.0/68.2 (13.9/62.7)
TS16			C_1	1.94	3SiO	GS23	-3.2/14.3 (1.5/8.0)
TS17			C_1	1.94	IM1 (Si_2O_2 + SiO)	GS24	45.4/-1.9 (49.2/9.6)
TS18			C_s	1.93	3SiO	GS24	15.6/23.9 (8.8/29.2)

[a] Names of the structures. [b] V1 and V2 are two views of each transition state. [c] MP2 natural orbital occupation numbers. [d] GS[i] and GS[f] denote initial and final minima on the IRC path.

Figure 6. A schematic of the synthesis and isomerization of Si_3O_3.

There is an intermediate (IM1) on the reaction path Si_2O_2 + SiO → Si_3O_3. IM1 is 4.5 (8.8) kcal/mol lower in energy than the separated reactants at the CR-CCSD(T) (MP2) level of theory. There is no barrier between the reactants and IM1. The energy of formation of the lowest isomer GS18 from reactants (Si_2O_2 + SiO) is −56.6 and −50.2 kcal/mol at the CR-CCSD-

(T) and MP2 levels, respectively. This reaction occurs with no barrier if the reactants are separated by ~3 Å.

TS9 and TS17 connect IM1 with GS19 and GS24, respectively. The energy barrier for the former transformation is very small (Table 10), while that for the latter is more than 40 kcal/mol. So, IM1 is most likely to transform to GS19. An additional transition state may connect GS19 with global minimum GS18, but such a structure was not found. There is a "direct" transition state (TS13) for the reaction $Si_2O_2 + SiO \rightarrow Si_3O_3$ (SiO interacts with "triangle" Si_2O_2 isomer) that does not require passing through an intermediate structure. The CR-CCSD(T) barrier for this reaction is only 15.5 kcal/mol, but the product is isomer GS27. Since this isomer is very high in energy, it is probably not directly involved in the experimentally observed processes. Two transition states for the reaction $3SiO \rightarrow Si_3O_3$ (TS16 and TS18) (Figure 3) connect the reactants with GS23 and GS24, respectively. The $3SiO \rightarrow$ TS16 CR-CCSD(T) barrier is negative, and the CR-CCSD(T) barrier for $3SiO \rightarrow$ TS18 is 15.6 kcal/mol.

(h) Si_3O_4. The Si_3O_4 local minima and transition states are listed in Tables 10 and 11, respectively, and a schematic of the PES is shown in Figure 7 . The singlet GS29 is predicted by both MP2 and CR-CCSD(T)//MP2 to be the lowest-energy isomer. The singlet−triplet splitting for the lowest singlet and triplet states is 64.5 kcal/mol. All isomers except GS36 have MP2 HOMO NOON in the range of 1.91−1.95. For GS36, the HOMO NOON is 1.81, indicating significant multi-configurational character.

TS20 is predicted by both MP2 and CR-CCSD(T)/MP2 to be the lowest-energy transition state. For all TSs, excluding TS21, the MP2 HOMO NOON are in the range 1.91−1.95. TS21 has the MP2 HOMO NOON = 1.87.

The search for intermediates and transition states has shown that there is an intermediate structure IM2 for the reaction $Si_2O_3 + SiO \rightarrow Si_3O_4$ (GS29, planar rhombic isomer of Si_2O_3, Figure 4). The CR-CCSD(T) (MP2) energy of formation for GS29 is −10.8 (−11.8) kcal/mol. There are two reaction paths for the formation of the global minimum isomer GS29. The first of these connects the intermediate IM2 with GS36 through transition state TS19; this is followed by isomerization of GS36 to GS29 through TS22. The second route connects IM2 with GS30 through the transition state TS28 and GS30 with GS29 through TS20. The second route is preferable due to the lower energy barriers on the reaction path. No barrier has been detected that connects IM2 with the reactants. The transition states TS21, TS23, TS24, TS25, TS26, and TS27 describe a set of isomerization reactions of Si_3O_4 clusters.

IV. Conclusions

Only the largest Si_3O_3 and Si_3O_4 clusters appear to have intermediate structures and transition states on the reaction paths leading to formation of these Si_mO_n clusters.

Reactions of formation of smaller Si_mO_n clusters (Si_2O_2, Si_2O_3, and Si_2O_4) are all barrierless processes. The previous study[20] on the formation of SiO and SiO_2 also showed that these reactions occur with no reaction barrier. This leads to the conclusion that small Si−O clusters have a strong thermodynamic driving force for "growing" into bigger clusters. This has also been noted in a recent paper by Zhang et al.[44] It may be anticipated that as the values of *m* and *n* increase, one will find an increasingly complex energy landscape, with intermediates and transition states.

For most of the species studied here, single configuration methods appear to be reasonable, so methods such as MP2 and

TABLE 10: Structures and Energies of Isomers of Si_3O_4

Isomer[a]	Structure[b] V1	Structure[b] V2	CR CCSD(T) relative energy (MP2) (kcal/mol)	Point Group	MP2 HOMO NOON[c]
GS29			0.0 (0.0)	C_{2v}	1.95
GS30			28.9 (30.1)	C_{2v}	1.95
GS31			42.7 (37.1)	C_s	1.95
GS32			63.4 (59.7)	C_s	1.94
GS33			69.9 (67.3)	C_s	1.95
GS34			72.2 (60.8)	C_{2v}	1.94
GS35			74.7 (68.2)	C_{2v}	1.94
GS36			75.5 (48.0)	C_{2v}	1.81
GS37			84.1 (80.3)	C_s	1.94
GS38			125.8 (117.2)	C_1	1.94
GS39			127.8 122.5)	C_{2v}	1.91
GS40			131.1 (117.4)	C_{2v}	1.93
GS41			135.6 (127.3)	C_1	1.91
GS42			145.7 (140.4)	C_1	1.92
GS43			146.5 (137.2)	C_1	1.91
GS44			147.1 (137.4)	C_s	1.92
IM2			76.5 (67.2)	C_s	1.95

[a] Names of the isomers. [b] V1 and V2 are two views of each isomer. [c] MP2 natural orbital occupation numbers. [d] IM1 indicates $SiO + Si_2O_2$ intermediate structure.

TABLE 11: Structures, Energies, and Reaction Paths for Si_3O_4[d]

TS[a]	Structure[b] V1	Structure[b] V2	Point Group	MP2 HOMO NOON[c]	GS[i]	GS[f]	Barrier height, (kcal/mol) GS^i/GS^f CR-CCSD(T) (MP2)
TS19			C_s	1.95	IM2 (Si_2O_3 + SiO)	GS36	0.0/1.0 (0.0/19.2)
TS20			C_s	1.94	GS30	GS29	30.7/59.6 (22.8/52.9)
TS21			C_{2v}	1.87	GS39	GS36	17.3/70.3 (18.2/92.7)
TS22			C_s	1.94	GS29	GS36	62.1/-13.4 (56.5/8.5)
TS23			C_1	1.92	GS30	GS35	73.1/27.3 (64.1/25.9)
TS24			C_s	1.92	GS41	GS44	10.9/-0.5 (10.3/0.1)
TS25			C_1	1.94	GS32	GS37	61.6/40.9 (57.7/37.1)
TS26			C_1	1.91	GS39	GS43	17.5/-1.2 (16.2/1.4)
TS27			C_1	1.92	GS41	GS39	-0.5/7.3 (5.3/10.1)
TS28			C_1	1.95	IM2 Si_2O_3 +SiO	GS30	0.7/48.3 (0.4/37.5)

[a] Names of the structures. [b] V1 and V2 are two views of each transition state. [c] MP2 natural orbital occupation numbers. [d] GS^i and GS^f denote initial and final minima on the IRC path.

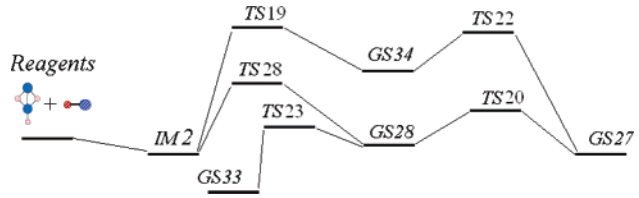

Figure 7. A schematic of the synthesis and isomerization of Si_3O_4.

CR-CCSD(T) are appropriate. Only a few stationary points may require MCSCF-based wave functions.

The MP2/6-31G(d) optimizations of Si_mO_n cluster geometries presented here have added some new low- and high-energy isomers of Si_mO_n clusters in comparison with the B3LYP/6-31G(d) calculations of ref 19. However, the relative energies for the structure of isomers that are common to both studies are very similar, so the B3LYP geometries for the closed-shell species appear to be reliable. The primary new features presented here are the exploration of higher spin states (important for some species) and an analysis of the reaction pathways for each species. It has, for example, been shown that all isomers of the Si_2O_5, Si_3O, Si_3O_3, and Si_3O_4 clusters have singlet global minima, while the Si_3O_2 cluster has a triplet ground state.

In general, the Si_mO_n clusters have very complex potential energy surfaces, with multiple low-lying spin states. So, an adequate level of theory is required to provide a quantitatively meaningful broad picture of their behavior. It appears that B3LYP can provide reasonable geometries, at least for closed-shell species, and that the MP2 relative energies are at least in qualitative agreement with those based on coupled cluster methods.

Acknowledgment. The authors are grateful to Professor Piotr Piecuch for invaluable discussions. The study has been supported in part by grants from the U.S. Department of Energy via the Ames Laboratory and the Air Force Office of Scientific Research.

References and Notes

(1) Wang, N.; Tang, Y. H.; Zhang, Y. F.; Lee, C. S.; Lee, S. T. *Phys. Rev.* **1998**, *B58*, R16024.
(2) Wang, N.; Tang, Y. H.; Zhang, Y. F.; Lee, C. S.; Bello, I.; Lee, S. T. *Chem. Phys. Lett.* **1999**, *299*, 237.
(3) Shi, W. S.; Peng, H. Y.; Zheng, Y. F.; Wang, N.; Shang, N. G.; Pan, Z. W.; Lee, C. S. *Adv. Mater.* **2000**, *12*, 1343.
(4) Sun, X. H.; Li, C. P.; Wong, W. K.; Wong, N. B.; Lee, C. S.; Lee, S. T.; Teo, B. K. *J. Am. Chem. Soc.* **2002**, *124*, 14464.
(5) Li, C. P.; Sun, X. H.; Wong, N. B.; Lee, C. S.; Lee, S. T.; Teo, B. K. *J. Phys. Chem. B* **2002**, *106*, 6980.
(6) Wang, L. S.; Desai, S. R.;Wu, H.; Nicholas, J. B. *Z. Phys. D* **1997**, *40*, 36.
(7) Fan, J.; Nicholas, J. B.; Price, J. M.; Colson, S. D.; Wang, L. S. *J. Am. Chem. Soc.* **1995**, *117*, 5417.
(8) Wang, L. S.; Wu, H.; Desai, S. R.; Fan, J.; Colson, S. D. *J. Phys. Chem.* **1996**, *100*, 8697.
(9) Wang, L. S.; Nicholas, J. B.; Dupuis, M.; Wu, H.; Colson, S. D. *Phys. Rev. Lett.* **1997**, *78*, 4450.
(10) Chelikowsky, J. R. *Phys. Rev.* **1998**, *B57*, 3333.
(11) Boldyrev, A. I.; Simons, J. *J. Phys. Chem.* **1993**, *97*, 5875.
(12) Sommerfeld, T.; Scheller, M. K.; Cederbaum, L. S. *J. Chem. Phys.* **1996**, *104*, 1464.
(13) Zhang, R. Q.; Chu, T. S.; Cheung, H. F.; Wang, N.; Lee, S. T. *Phys. Rev.* **2001**, *B64*, 113304.
(14) Chu, T. S.; Zhang, R. Q.; Cheung, H. F. *J. Phys. Chem. B* **2001**, *105*, 1705.
(15) Goldberg, N.; Iraqi, M.; Koch, W.; Schwarz, H. *Chem. Phys. Lett.* **1994**, *225*, 404.
(16) Nayak, S. K.; Rao, B. K.; Khanna, S. N.; Jena, P. *J. Chem. Phys.* **1998**, *109*, 1245.
(17) Sommerfeld, T.; Scheller, M. K.; Cederbaum, L. S. *J. Chem. Phys.* **1995**, *103*, 1057.
(18) Dupuis, M.; Nicholas, J. B. *Mol. Phys.* **1999**, *96*, 549.
(19) Lu, W. C.; Wang, C. Z.; Nguyen, V.; Schmidt, M. W.; Gordon, M. S.; Ho, K. M. *J. Phys. Chem. A* **2003**, *107*, 6936.
(20) Adamovic, I.; Gordon, M. S. *J. Phys. Chem. A* **2004**, *108*, 8395.
(21) Møller, C.; Plesset, M. S. *Phys. Rev.* **1934**, *46*, 618.
(22) Hehre, W. J.; Ditchfield, R.; Pople, J. A. *J. Chem. Phys.* **1972**, *56*, 2257. Francl, M. M.; Petro, W. J.; Hehre, W. J.; Binkley, J. S.; Gordon, M. S.; DeFrees, D. J.; Pople, J. A. *J. Chem. Phys.* **1982**, *77*, 3654.
(23) Becke, A. D. *Phys. Rev.* **1988**, *A38*, 3098. Lee, C.; Yang, W.; Parr, R. G. *Phys. Rev.* **1988**, *B37*, 785.
(24) Curtiss, L. A.; Pople, J. A.; Raghavachari, K. *J. Chem. Phys.* **1993**, *98*, 1293.
(25) (a) Bernstein, R. J.; Scheiner, S. *Int. J. Quantum Chem.* **1986**, *29*, 1191. (b) Schnöckel, H.; Mehner, T.; Plitt, H. S.; Schunck, S. *J. Am. Chem. Soc.* **1989**, *111*, 4578. (c) Bencivenni, L.; Pelino, M.; Ramondo, F. *J. Mol. Struct.* (*THEOCHEM*) **1992**, *253*, 109. (d) Friesen, M.; Junker, M.; Zumbusch, A.; Schnöckel, H. *J. Chem. Phys.* **1999**, *111*, 7881.
(26) Snyder, L. C.; Raghavachari, K. *J. Chem. Phys.* **1984**, *80*, 5076.
(27) (a) Nagase, S.; Kudo, T. *Organometallics* **1987**, *6* (11), 2456. (b) Nagase, S.; Kudo, T.; Kurakake, T. *J. Chem. Soc., Chem. Commun.* **1988**, 1063.
(28) Schmidt, M. W.; Nguyen, K. A.; Gordon, M. S.; Montgomery, J. A., Jr. *J. Am. Chem. Soc.* **1991**, *113*, 5998.
(29) Nguyen, K. A.; Carroll, M. T.; Gordon, M. S. *J. Am. Chem. Soc.* **1991**, *113*, 7924.
(30) Wang, L.-S.; Wu, H.; Desai, S. R.; Fan, J.; Colson, S. D. *J. Phys. Chem.* **1996**, *100*, 8697.
(31) Ystenes, M. *Spectrochim. Acta* **1994**, *50A*, 219.
(32) Schmidt, M. W.; Baldridge, K. K.; Boatz, J. A.; Elbert, S. T.; Gordon, M. S.; Jensen, J. H.; Koseki, S.; Matsunaga, N.; Nguen, K. A.; Su, S.; Windus, T. L.; Dupuis, M.; Montgomery, J. A. *J. Comput. Chem.* **1993**, *14*, 1347.
(33) (a) Becke, A. D. *Phys. Rev. A* **1988**, *38*, 3098. (b) Lee, C.; Yang, W.; Parr, R. G. *Phys. Rev. B* **1988**, *37*, 785. (c) For the specific flavor of

the B3LYP used, consult GAMESS manual: http://www.msg.ameslab.gov/GAMESS/ doc.menu.html.

(34) Piecuch, P.; Kucharski, S. A.; Kowalski, K.; Musial, M. *Comput. Phys. Commun.* **2002**, *149*, 71.

(35) Dunning, T. H., Jr. *J. Chem. Phys.* **1989**, *90*, 1007.

(36) Woon, D. E.; Dunning, T. H., Jr. *J. Chem. Phys.* **1993**, *98*, 1358.

(37) (a) Nakano, H. *J. Chem. Phys.* **1993**, *99*, 7983. (b) Hirao, K. *Chem. Phys. Lett.* **1992**, *190*, 374.

(38) (a) Hunt, W. J.; Hay, P. J.; Goddard, W. A. *J. Chem. Phys.* **1972**, *57*, 738. (b) Hay, P. J.; Hunt, W. J.; Goddard, W. A. *J. Am. Chem. Soc.* **1972**, *94*, 8293. (c) Goddard, W. A.; Dunning, T. H.; Hunt, W. J.; Hay, P. J. *Acc. Chem. Res.* **1973**, *6*, 268.

(39) Gonzales, C.; Schlegel, B. H. *J. Phys. Chem.* **1990**, *94*, 5523.

(40) Pulay, P.; Hamilton, T. P. *J. Chem. Phys.* **1988**, *88*, 4926. Gordon, M. S.; Schmidt, M. W.; Chaban, G. M.; Glaesemann, K. R.; Stevens, W. J.; Gonzalez, C. *J. Chem. Phys.* **1999**, *110*, 4199.

(41) *CRC Handbook of Chemistry and Physics*, 84th ed.; Lide, D. R., Ed.; CRC Press: Boca Raton, FL, 2002.

(42) Andersono, J. S.; Ogden, J. S. *J. Chem. Phys.* **1969**, *51*, 4189.

(43) Zachariah, M. R.; Tsang, W. *J. Phys. Chem.* **1995**, *99*, 5308.

(44) Zhang, R. Q.; Zhao, M. W.; Lee, S. T. *Phys. Rev. Lett.* **2004**, *93*, 099503.